*Rev. Mexicana Astron. Astrof.*, **22**, 19-25 (1991)

# RADIO OBSERVATIONS OF H II REGIONS WITH NARROW RADIO RECOMBINATION LINES

P. Planesas[1], J. Gómez-González[1]
L. F. Rodríguez[2] and J. Cantó[2]

*Received 1990 May 14*

RESUMEN

Reportamos observaciones de las líneas de recombinación H110$\alpha$ y H138$\beta$ y de la transición rotacional J = 1 – 0 del CO hacia regiones H II que se sospechaba, a partir de resultados de encuestas con cociente de señal a ruido modesto, tuvieran líneas de recombinación muy angostas. Solo una de las fuentes estudiadas, G0.6–0.6, tiene líneas anómalamente angostas, $\Delta v$(H110$\alpha$) $\simeq$ 14.4±0.4 km s$^{-1}$. Sin embargo, como grupo, las fuentes estudiadas por nosotros tienen líneas sistemáticamente más angostas que las regiones H II "típicas". G0.6–0.6 y G19.5+0.1 son también notables porque sus líneas tienen un componente "turbulento" muy pequeño. Otra región H II en la muestra, G19.6–0.1, parece haber creado una cavidad tipo ampolla en la nube molecular asociada. No hay diferencias obvias entre nuestra muestra seleccionada de asociaciones región H II-nube molecular y otras muestras más amplias estudiadas por otros autores.

ABSTRACT

We report observations of the H110$\alpha$ and H138$\beta$ recombination lines and of the J = 1 – 0 rotational transition of CO toward H II regions suspected of having narrow radio recombination lines from the results of surveys with modest signal-to-noise ratio. Only one of the sources studied, G0.6–0.6, was found to have anomalously narrow recombination line emission, $\Delta v$(H110$\alpha$) $\simeq$ 14.4±0.4 km s$^{-1}$. However, as a group, the sources studied by us have lines that are systematically narrower than "typical" H II regions. G0.6–0.6 and G19.5+0.1 are also unusual in having very little "turbulent" broadening in their recombination line emission. Another H II region in our sample, G19.6–0.1, seems to have created a blister-like cavity in its associated molecular cloud. There is no obvious difference between our selected sample of H II region-molecular cloud associations and the larger samples studied by others.

*Key words:* **NEBULAE-H II REGIONS – RADIO SOURCES-LINES**

## I. INTRODUCTION

Radio recombination lines from galactic H II regions usually have half-power full widths, $\Delta v$, in the range of 25 to 35 km s$^{-1}$ (Garay and Rodríguez 1983). During a survey of H II regions, Shaver, McGee and Pottasch (1979) detected two sources, G339.1–0.2 and RCW 94, with unusually narrow line widths, $\Delta v \simeq 15.0$ km s$^{-1}$. We will refer to these sources as narrow-line H II regions. Two additional narrow-line H II regions, G0.6–0.6 and S59, were later reported by Shaver *et al.* (1983). In his 3-cm radio recombination line survey of nearly 500 continuum sources, Lockman (1989) reports 11 narrow-line H II regions. These remarkable sources have two important properties. The first is that they are relatively cold for an H II region; the line width alone implies electron temperatures of 5000 K or less. These low values for the electron temperature are confirmed by the values derived from radio recombination line and optical forbidden line observations (Shaver *et al.* 1983). These low electron temperatures can, however, be understood if the nebula is very rich in the cooling heavy elements. The second property is quite puzzling and remains unexplained; while typical H II regions have a sizable "turbulent" component in their line widths, the width of these narrow-line H II regions seems to be mostly thermal.

In this paper we present radio recombination line (H110$\alpha$ and H138$\beta$) and carbon monoxide (J = 1–0) observations of a selected sample of H II regions that were suspected of having narrow recombination line emission.

## II. SOURCE SELECTION AND OBSERVATIONS

At the time we started this study (1982), the only narrow-line H II regions known were G339.1−0.2 and RCW 94, two southern objects that could not be studied adequately from the northern hemisphere. We decided to search for more northern objects adopting the following approach. From the survey of Downes *et al.* (1980) we selected all sources with reported $\Delta v \leq 18$ km s$^{-1}$. The 15 sources selected are listed in Table 1, together with the line widths determined by Downes *et al.* (1980) and an indication of whether or not they were observed by us in CO and radio recombination lines. The typical uncertainty in the determination of $\Delta v$ in the survey of Downes *et al.* was several km s$^{-1}$. This implied that to establish these sources as *bona fide* narrow-line H II regions, spectra with much better signal-to-noise ratio was required.

We carried out observations of the H110$\alpha$ and H138$\beta$ radio recombination lines during 1985

TABLE 1

SOURCES WITH $\Delta v \leq 18$ km s$^{-1}$ IN DOWNES *ET AL.* (1980)

| Source | $\alpha$ (1950) | $\delta$ | $\Delta v$ (km s$^{-1}$) | Observed in CO? | RRL? |
|---|---|---|---|---|---|
| G0.6–0.6 | 17 46 15.2 | −28 45 25 | 15 | Y | Y |
| G0.6–0.5 | 17 45 47.8 | −28 40 31 | 13 | Y | Y |
| G13.9+0.3 | 18 11 41.9 | −16 46 28 | 17 | N | Y |
| G14.4–0.7 | 18 16 15.7 | −16 43 19 | 18 | N | N |
| G18.2–0.4 | 18 22 40.7 | −13 18 31 | 16 | Y | Y |
| G19.5+0.1 | 18 23 15.3 | −11 54 36 | 15 | N | Y |
| G19.6–0.1 | 18 24 28.6 | −11 55 23 | 17 | Y | Y |
| G23.0–0.4 | 18 31 41.1 | −09 03 00 | 18 | N | N |
| G23.3–0.3 | 18 31 52.9 | −08 46 06 | 17 | N | N |
| G39.3–0.1 | 19 00 44.7 | 05 31 21 | 18 | Y | Y |
| G48.6+0.2 | 19 17 32.7 | 13 57 26 | 18 | Y | Y |
| G49.4–0.5 | 19 21 36.9 | 14 19 41 | 18 | Y | Y |
| G50.1–0.7 | 19 23 43.1 | 14 50 03 | 17 | N | N |
| G54.1–0.1 | 19 29 30.3 | 18 36 01 | 16 | Y | Y |
| G59.8+0.2 | 19 40 26.6 | 23 42 43 | 18 | Y | Y |

TABLE 2

PARAMETERS OF OBSERVED RADIO RECOMBINATION LINES

| Source | | | H110$\alpha$ | | | H138$\beta$ | | |
|---|---|---|---|---|---|---|---|---|
| | $T_C$ (K) | $\theta_S$ ($'$) | $T_L$ (mK) | $\Delta v$ (km s$^{-1}$) | $v_{lsr}$ (km s$^{-1}$) | $T_L$ (mK) | $\Delta v$ (km s$^{-1}$) | $v_{lsr}$ (km s$^{-1}$) |
| G0.6–0.6 | 3.8 | 5.4 | 732±18 | 14.4±0.4 | 16.8±0.2 | 171±14 | 22.4±2.1 | 17.8 ±0.9 |
| G0.6–0.5 | 1.1 | 4.7 | 406±9 | 17.5±0.4 | 19.3±0.2 | 89±5 | 22.2±1.4 | 20.0 ±0.6 |
| G13.9+0.3 | 6.4 | 3.0 | 591±9 | 23.3±0.4 | 50.3±0.2 | 126±9 | 22.7±1.8 | 49.8 ±0.8 |
| G18.2–0.4 | 2.9 | 4.7 | 298±8 | 23.3±0.4 | 50.3±0.2 | 126±9 | 22.7±1.8 | 49.8 ±0.8 |
| G19.5+0.1 | 2.4 | 4.0 | 215±8 | 18.1±0.8 | 19.9±0.3 | 69±9 | 15.7±2.4 | 19.6 ±1.0 |
| G19.6–0.1 | 2.2 | 5.9 | 241±8 | 22.6±0.8 | 57.0±0.3 | 89±8 | 15.7±1.7 | 56.5 ±0.7 |
| G39.3–0.1 | 3.0 | 3.7 | 177±7 | 24.6±1.1 | 21.7±0.4 | 51±6 | 29.8±4.3 | 24.5 ±1.8 |
| G48.6+0.2 | 1.7 | 4.5 | 170±4 | 19.1±0.6 | 9.7±0.2 | 51±5 | 19.0±2.1 | 9.8 ±0.9 |
| G49.4–0.5 | 2.2 | 3.6 | 279±5 | 20.7±0.5 | 58.4±0.2 | 69±4 | 26.0±1.9 | 58.4 ±0.8 |
| G54.1–0.1 | 2.1 | 3.8 | 192±7 | 21.9±0.9 | 41.7±0.4 | 64±7 | 20.9±2.7 | 41.4 ±1.1 |
| G59.8+0.2 | 1.5 | 3.1 | 104±4 | 24.0±1.2 | −3.1±0.5 | 34±6 | 19.1±3.9 | −2.9 ±1.6 |

February using the Max-Planck-Institut für Radioastronomie 100-m radio telescope located at Effelsberg, FRG. At the observing frequency of 4.874 GHz the HPBW was 2.9 arcmin and the aperture and beam efficiencies were 0.47 and 0.65, respectively. The receiver was a cooled parametric amplifier followed by a 1024 channel digital autocorrelator. We divided the autocorrelator into two 512 channel spectrometers, each with a total bandwidth of 6.25 MHz. One spectrometer was centered on the H110$\alpha$ line and the other on the H138$\beta$ line. The observations were made using position switching and 5-minute integrations. The line parameters for the sources observed, determined from a least-squares Gaussian fit, are given in Table 2. The peak continuum temperature of each source was determined from scans across the peak of the source and its value is given also in Table 2. To determine this peak continuum temperature we subtracted, when required, a background contribution estimated from the scans. In Table 2 we also give the HPFW angular size of the H II regions, taken as the geometric mean of the values obtained in right ascension and declination. These angular sizes are convolved with the antenna beam. Our line and continuum parameters are in good agreement with the values reported by Altenhoff *et al.* (1978) and Downes *et al.* (1980). However, our observations have much better signal-to-noise ratio since we concentrated on a small number of sources.

The observations of the J = 1–0 rotational transition of CO were made in 1983 October and 1984 July using the 4.9-m radio telescope of the Millimeter Wave Observatory of the University of Texas. At the observing frequency of 115.271 GHz the antenna had a HPBW of 2.3 arcmin and a beam efficiency of 0.7. The receiver was a cooled Schottky mixer and the spectrometer a 264-channel filter bank. The channel width was 250 kHz, for a velocity resolution of 0.65 km s$^{-1}$ and a velocity coverage of 172 km s$^{-1}$. The observations were made with position switching and 5-minute integrations. We mapped the sources indicated in Table 3, observing typically 30 to 40 positions and using full beam intervals. CO spectra toward the inner Galaxy show components at various velocities. We have assumed that the component with radial velocity closest to that of the H II region arises from an associated molecular cloud. In all cases this component is the strongest in the CO spectrum, a result that gives support to our assumption that it is this component the one which is associated with the H II region. We fitted Gaussian profiles to the CO spectra and made maps of the integrated line intensity of the CO component associated with the H II region. These maps are shown in Figures 1 to 8. The radial velocities of these components are given in Table 3, together with those of the H110$\alpha$ recombination lines measured by us. The rms dispersion of the velocity difference is 2.1 km s$^{-1}$, very similar to the value of 2.8 km s$^{-1}$ found by Waller *et al.* (1987) for a sample of 54 H II region-molecular cloud associations.

TABLE 3

H110$\alpha$ AND CO RADIAL LSR VELOCITIES

| Source | $v_{lsr}$ (H II) (km s$^{-1}$) | $v_{lsr}$ (CO) (km s$^{-1}$) | $v_{lsr}$ (H II) – $v_{lsr}$ (CO) (km s$^{-1}$) |
|---|---|---|---|
| G0.6–0.6 | 16.8 | 16.6 | 0.2 |
| G0.6–0.5 | 19.3 | 17.3 | 2.0 |
| G18.2–0.4 | 44.2 | 49.1 | –4.9 |
| G19.6–0.1 | 57.0 | 58.1 | –1.1 |
| G39.3–0.1 | 21.7 | 21.8 | –0.1 |
| G48.6+0.2 | 9.7 | 11.4 | –1.7 |
| G49.4–0.5 | 58.4 | 59.3 | –0.9 |
| G54.1–0.1 | 41.7 | 39.3 | 2.4 |
| G59.8+0.2 | –3.1 | –2.9 | –0.2 |

## III. DISCUSSION

In 10 of the 11 sources observed by us in the H110$\alpha$ line (see Table 2), we measured broader widths than those reported by Downes *et al.* (1980). The exception is G0.6–0.6, where we determined a remarkably narrow width, $\Delta v \simeq 14.4$ km s$^{-1}$. This source is one of the two sources reported previously by Shaver *et al.* (1983) and the northernmost of the four narrow-line H II regions known before the survey of Lockman (1989). Nevertheless, as a class, the sources studied by us have narrower lines than typical H II regions, since they fall below the usual range for $\Delta v$, which is 25 to 35 km s$^{-1}$ (Garay and Rodríguez 1983). Assuming LTE and that the ionized helium to ionized hydrogen ratio is 0.08 we derived, from the continuum and H110$\alpha$ observations, the electron temperatures given in Table 4. The LTE assumption seems reasonable since, as shown also in Table 4, the integrated $\beta/\alpha$ ratio is generally close to the expected LTE value of 0.28, suggesting no large departures from LTE. One of the sources, G0.6–0.5, seems to have an unusually low electron temperature. At present it is unclear if this is a real effect or if it can be attributed to an observational problem (for example, to an improper subtraction of the baseline in the continuum scans, leading to an underestimate of the continuum). In fact, Downes *et al.* (1980) give a larger continuum temperature for this source. In this table we also give the Doppler temperature, $T_D$, derived from the observed width

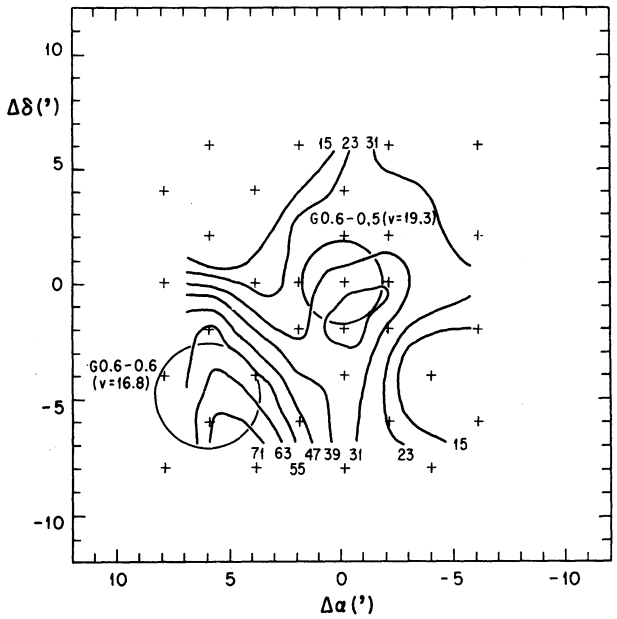


Fig. 1. The solid contours are the integrated intensities (K km $s^{-1}$) for the CO component closest to the velocity of the H II region G0.6–0.5. The integrated intensity for each contour is given in the figure. The position and approximated extent of the H II regions in the zone are indicated with a circle. Next to the name of the H II region we also give its radial velocity with respect to the LSR. The small crosses mark the positions observed in CO. The figure center is at the position for G0.6–0.5 given in Table 1.

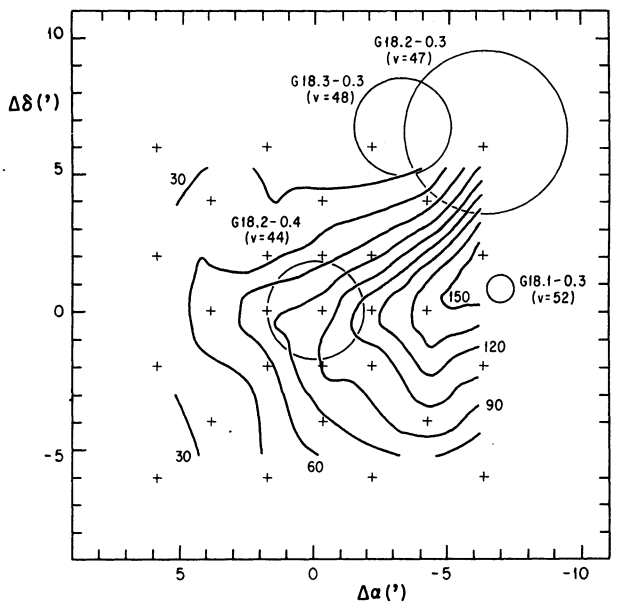


Fig. 2. Same as Figure 1, but for G18.2–0.4.

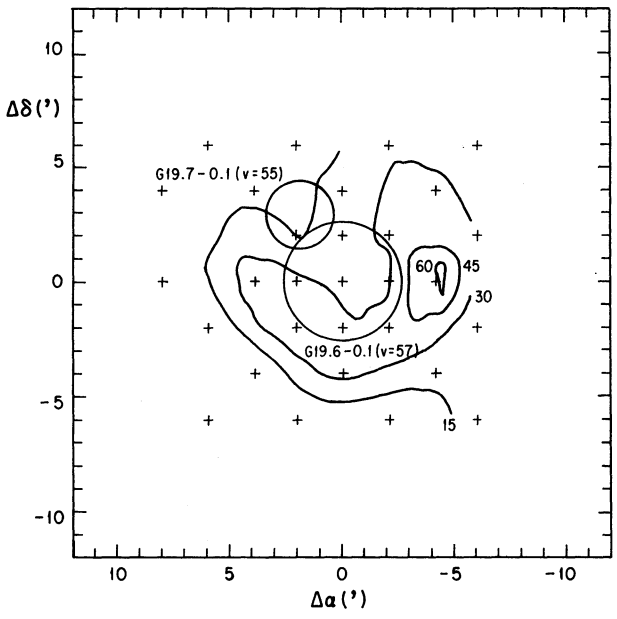


Fig. 3. Same as Figure 1, but for G19.6–0.1.

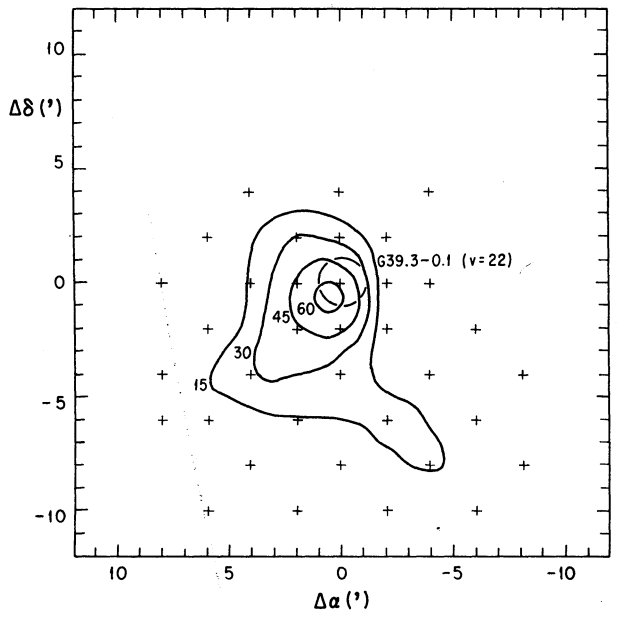


Fig. 4. Same as Figure 1, but for G39.3–0.1.

of the H110$\alpha$ line, as well as the "turbulent" width, $\Delta v_{TUR}$, which is obtained from

$$\Delta v_{TUR} = (\Delta v_{TOT}^2 - \Delta v_{THER}^2)^{0.5},$$

where $\Delta v_{TOT}$ is the total width observed and $\Delta v_{THER}$ is the width implied from $T_e$. In Table

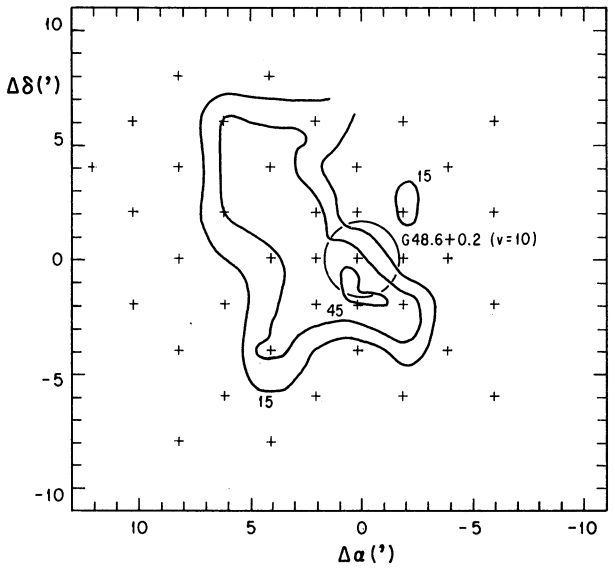


Fig. 5. Same as Figure 1, but for G48.6+0.2.

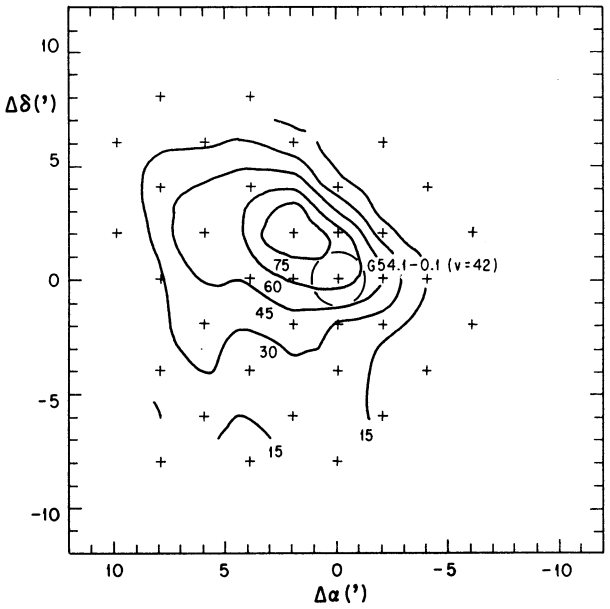


Fig. 7. Same as Figure 1, but for G54.1–0.1.

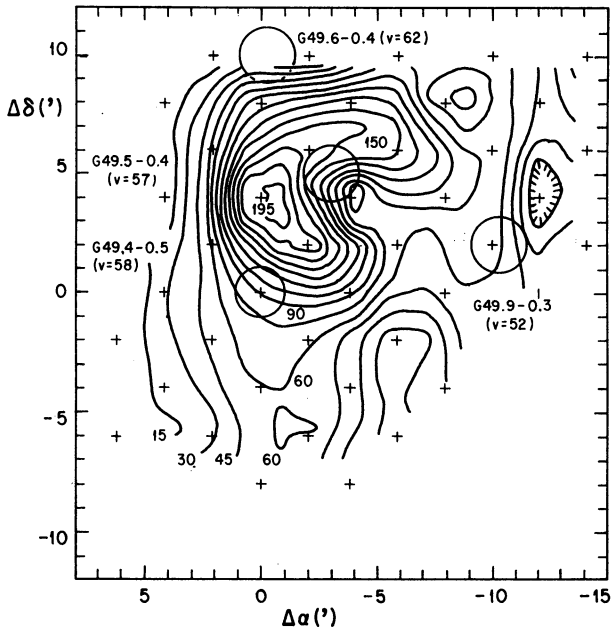


Fig. 6. Same as Figure 1, but for G49.4–0.5.

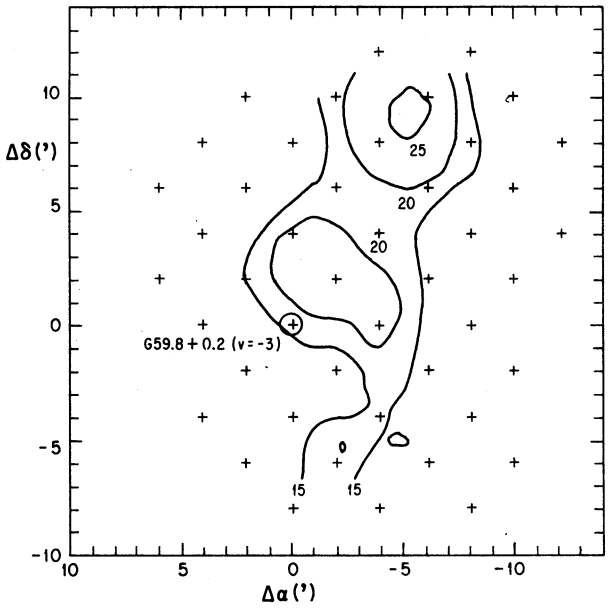


Fig. 8. Same as Figure 1, but for G59.8+0.2.

4 we also give the diameter, the lower limits for the electron densities, and the required ionizing rates of these H II regions. These parameters were obtained following the formulation of Schraml and Mezger (1969). The criteria used to obtain the distances given in Table 4 are described in detail by Planesas (1987). Typically, these H II regions are large (with diameters of $\sim$ 10 pc), of low electron density ($n_e \sim 10^2$ cm$^{-3}$) and have large ionizing rates that require one or more early O-type star(s).

Two of the H II regions observed, G0.6–0.6 and G19.5+0.1, appear to have very small "turbulent" components, $\Delta v_{TUR} \leq 7.0$ km s$^{-1}$. The other H II regions have $\Delta v_{TUR}$ values in the range of 11 to 18

TABLE 4

DERIVED PARAMETERS FOR THE OBSERVED H II REGIONS

| Source | Distance (kpc) | H138$\beta$/H110$\alpha$ | $T_e^*$ (H110$\alpha$) (K) | $T_D$ (H110$\alpha$) (K) | $\Delta v_{TUR}$ (km s$^{-1}$) | Diam. (pc) | Electron Density (cm$^{-3}$) | Required Ionizing Rate (s$^{-1}$) |
|---|---|---|---|---|---|---|---|---|
| G0.6–0.6 | 10.0 | 0.37±0.05 | 3900±600 | 4500±300 | 5±1 | 13 | $\geq$ 60 | $6.6\times10^{49}$ |
| G0.6–0.5 | 10.0 | 0.28±0.03 | 1800±300 | 6700±300 | 15±2 | 11 | $\geq$ 40 | $1.5\times10^{49}$ |
| G13.9+0.3 | 5.3 | 0.20±0.02 | 4800±700 | 11800±400 | 18±2 | 1 | $\geq$800 | $1.0\times10^{49}$ |
| G18.2–0.4 | 4.2 | 0.28±0.04 | 5000±800 | 8900±600 | 14±2 | 5 | $\geq$ 90 | $7.0\times10^{48}$ |
| G19.5+0.1 | 16.8 | 0.28±0.06 | 6200±900 | 7100±600 | 7±1 | 14 | $\geq$ 50 | $6.5\times10^{49}$ |
| G19.6–0.1 | 4.9 | 0.28±0.05 | 4300±600 | 11100±800 | 18±2 | 7 | $\geq$ 60 | $1.2\times10^{49}$ |
| G39.3–0.1 | 14.0 | 0.35±0.07 | 6800±1000 | 13100±1200 | 17±2 | 9 | $\geq$ 80 | $5.1\times10^{49}$ |
| G48.6+0.2 | 12.5 | 0.30±0.04 | 5300±800 | 8000±500 | 11±1 | 13 | $\geq$ 50 | $3.3\times10^{49}$ |
| G49.4–0.5 | 7.5 | 0.31±0.03 | 4000±600 | 9300±500 | 16±2 | 5 | $\geq$110 | $1.0\times10^{49}$ |
| G54.1–0.1 | 8.0 | 0.32±0.06 | 5100±800 | 10500±900 | 16±2 | 6 | $\geq$ 90 | $1.2\times10^{49}$ |
| G59.8+0.2 | 10.3 | 0.26±0.07 | 5900±900 | 12600±1300 | 18±2 | 3 | $\geq$170 | $9.0\times10^{48}$ |

TABLE 5

PARAMETERS OF ASSOCIATED MOLECULAR CLOUDS

| Source | Radius (pc) | $\Delta v_{CO}$ (km s$^{-1}$) | $M_{CO}$ ($M_\odot$) | $M_{VIR}$ ($M_\odot$) |
|---|---|---|---|---|
| G0.6–0.6[a] | 15 | 10 | $1\times10^5$ | $3\times10^5$ |
| G18.2–0.4 | > 7 | 11 | $>6\times10^4$ | $>2\times10^5$ |
| G19.6–0.1 | > 9 | 6 | $>4\times10^4$ | $>7\times10^4$ |
| G39.3–0.1 | 15 | 9 | $2\times10^5$ | $3\times10^5$ |
| G48.6+0.2 | 17 | 10 | $2\times10^5$ | $4\times10^5$ |
| G49.5–0.5 | >19 | 12 | $>5\times10^5$ | $>6\times10^5$ |
| G54.1–0.1 | >16 | 9 | $>2\times10^5$ | $>3\times10^5$ |
| G59.8+0.2 | >14 | 4 | $>1\times10^5$ | $>5\times10^4$ |

a. This cloud also engulfs G0.6–0.5.

km s$^{-1}$, similar to the values listed by Labrandero *et al.* (1991) for other large, low-density galactic H II regions.

We now turn our attention to the results of the carbon monoxide mapping. In Table 5 we show the parameters of the associated molecular clouds. The characteristic size was taken as the geometric mean of the major and minor diameters, measured down to the level where the integrated CO intensity is 15 K km s$^{-1}$. We estimated masses for the clouds using an average of the formulae for the molecular hydrogen column density given by Bohlin *et al.* (1978), Liszt (1982), and Sanders *et al.* (1983), namely:

$$N(H_2) = 3\times10^{20}\int T_L(CO)dv \ ,$$

where $N(H_2)$ is in cm$^{-2}$, $T_L$ is in K, and $dv$ is in km s$^{-1}$. This column density is then integrated over the face of the cloud to derive the mass. An independent estimate for the molecular cloud mass can be obtained from virial arguments that give:

$$M_{VIR} \simeq 210\ R\ \Delta v^2 \ ,$$

where $M_{VIR}$ is the mass of the cloud in solar masses, R is the radius of the cloud in pc, and $\Delta v$ is the HPFW of the CO line. The sizes and estimated masses of the clouds are given in Table 5. The derived masses are typically $\sim 10^5\ M_\odot$, values characteristic of giant molecular clouds.

It is evident from inspection of Figures 1 to 8 that none of the H II regions appears projected against

the center of the molecular cloud. This is consistent with the results of Myers *et al.* (1986) and Waller *et al.* (1987), who found that, typically, H II regions appear displaced from the center of their associated molecular cloud by a few arcminutes.

The most interesting of our H II region-molecular cloud associations is that of G19.6–0.1, where this source and G19.7-0.1, another H II region in the zone, seem to have created a blister-type structure in the associated molecular cloud (see Figure 3). Observations of higher angular resolution are required to test this proposition.

We have noted that these H II region-molecular cloud associations do not appear to differ significantly from those discussed in the larger samples of Myers *et al.* (1986) and Waller *et al.* (1987). Then, why are the radio recombination lines systematically narrower? Labrandero *et al.* (1991) have discussed the behavior of radio recombination line width with size of the H II region. They find that the line width from H II regions decreases with increasing size. This decrease is caused by two effects: 1) as the H II region becomes bigger, it usually becomes less dense, and cooling via optical forbidden lines is more effective and, 2) as the density contrast between the H II region and the associated molecular cloud decreases, there are less "turbulent" motions. The H II regions studied by us are fairly large (with diameters typically in the 5 to 10 pc range) and this may account for the narrow line widths. However, it is clear that much more observational and theoretical work is needed to understand the origin of these differences between H II regions.

## IV. CONCLUSIONS

We studied radio recombination and carbon monoxide emission lines from several H II region-molecular cloud associations where the radio recombination lines from the H II region appeared to be narrower than in "typical" H II regions. Our main conclusions are the following:

1) Only one source, G0.6–0.6, was found to have an unusually narrow line width ($\Delta v \simeq 14.4$ km s$^{-1}$).

2) G0.6–0.6 and G19.5+0.1 appear to have very small "turbulent" contribution in their line widths; most of it can be attributed to thermal motions.

3) G19.6–0.1 is most probably a blister H II region.

4) We discussed the radial velocities and locations of the H II regions with respect to those of the associated molecular clouds. We did not find significant differences between our results and those obtained for larger samples of H II regions.

## REFERENCES

Altenhoff, W. J., Downes, D., Pauls, T., and Schraml, J. 1978, *Astr. and Ap. Suppl.*, **35**, 23.
Bohlin, R.C., Savage, B.D., and Drake, J.F. 1978, *Ap. J.*, **224**, 132.
Downes, D., Wilson, T. L., Bieging, J. H., and Wink, J. 1980, *Astr. and Ap. Suppl.*, **40** 379.
Garay, G. and Rodríguez, L. F. 1983, *Ap. J.*, **266**, 263.
Labrandero, M. J., Rodríguez, L. F., Cantó, J., and Garay, G. 1991, in preparation.
Liszt, H.S. 1982, *Ap. J.*, **262**, 198.
Lockman, F. J. 1989, *Astr. and Ap. Suppl.*, **71**, 469.
Myers, P. C., Dame, T. M., Thaddeus, P., Cohen, R. S., Silverberg, R. F., Dwek, E., and Hauser, M. G. 1986, *Ap. J.*, **301**, 398.
Planesas, P. 1987, Ph. D. Thesis, University of Madrid.
Sanders, D.B., Solomon, P.M., and Scoville, N.A. 1983, *Ap. J.*, **276**, 182.
Schraml, J. P. and Mezger, P. G. 1969, *Ap. J.*, **156**, 269.
Shaver, P. A., McGee, R. X. and Pottasch, S. R. 1979, *Nature*, **280**, 476.
Shaver, P. A., McGee, R. X., Newton, L. M., Danks, A. C. and Pottasch, S. R. 1983, *M. N. R. A. S.*, **204**, 53.
Waller, W. H., Clemens, D. P., Sanders, D. B., and Scoville, N. Z. 1987, *Ap. J.*, **314**, 397.

Jorge Cantó and Luis F. Rodríguez: Instituto de Astronomía, UNAM, Apartado Postal 70-264, 04510 México, D. F., México.
Jesús Gómez-González and Pere Planesas: Centro Astronómico de Yebes (IGN), Apartado 148, E-19080 Guadalajara, Spain.